

Mechanical Behavior of Oats: Specific Groat Characteristics and Relation to Groat Damage During Impact Dehulling

J. A. Engleson¹ and R. G. Fulcher^{1,2}

ABSTRACT

Cereal Chem. 79(6):790–797

Oat damage has negative effects on milling yield and finished product quality. Interrelationships among groat characteristics and mechanical behavior were analyzed to better understand groat damage caused by impact dehulling (ID). Regression of the natural logarithm (ln) of apparent stiffness (S_{\max}) on the contents of ferulic acid, syringic acid, and moisture suggests that ferulic acid or perhaps diferulate cross-links increase groat stiffness, and syringic acid or perhaps syringate derivatives and moisture decrease groat stiffness. Polymer cross-linking decreases extensibility, and moisture (a plasticizer) softens polymers. Regression of

ln of apparent toughness (T) on β -glucan and protein content implies that both polymers increase groat toughness. β -glucan is a cell-wall polymer, and the cell wall is known to confer toughness. The location of these polymers (perhaps concentrated in the bran) may also confer toughness. Regression of ln(ID) on moisture content, starch content, and T/S_{\max} suggests that moisture decreases impact damage (as does T/S_{\max}), and starch increases damage. Starch may act like filler, increasing stiffness and damage. According to the ratio of T/S_{\max} , groats must be tough but not too stiff for low levels of damage.

Oat damage caused by impact dehulling has negative effects on milling yield and finished product quality. For constant dehulling conditions, the preventative agents of damage are groat or hull characteristics, or both, though specific characteristics have not been completely identified. Groat damage is proportional to oat mass (Symons and Fulcher 1988); the proportionality constant appears to be a function of biological variability in the groat or hull or both. In terms of impact dehulling, the literature focuses on dehuller efficiency, the percentage of oat input-mass dehulled in one pass (Ganßmann and Vorwerk 1995), rather than groat damage.

Kernel morphology, hull content (the percentage of oat mass that is hull), and moisture content affect dehuller efficiency. Small kernels require higher angular velocity than large kernels to achieve the same dehuller efficiency (Ganßmann and Vorwerk 1995; Lapvetelainen et al 2001). Tertiary kernels are smaller than secondary kernels, which are smaller than primary kernels (Marshall and Shaner 1992). Considerable variation in kernel size also exists within a floret group (Peek and Poehlman 1949; Handel 2001). Tertiary kernel shape is generally rounder (more circular) than supernumerary kernels (Handel 2001), where roundness is measured by digital image analysis and defined as

$$\text{roundness} = \frac{(\text{object perimeter})^2}{4\pi(\text{object area})} \quad (1)$$

where circular objects have roundness equal to 1, and roundness approaches 1 as the kernel image becomes more circular. Handel (2001) showed that a high frequency of tertiary kernels results in smaller, less uniform, and rounder supernumerary kernels, and decreases efficiency of compressed air dehulling, which has positive correlations with impact dehulling (Doehlert et al 1999).

Many studies have shown that tertiary kernels have lower hull content than supernumerary kernels (Peek and Poehlman 1949; Wesenberg and Shands 1971; Youngs and Shands 1974; Pomeranz et al 1979; Palagy 1983; Lapvetelainen et al 2001). However, Ganßmann and Vorwerk (1995) demonstrated that dehuller efficiency is inversely proportional to hull content for constant moisture and dehuller conditions. This relationship suggests that the dehuller efficiency of tertiary kernels should be high, which is generally not true. The contradiction may indicate that hull content alone is not an adequate predictor of dehuller efficiency.

Dehuller efficiency also depends on moisture content (Ganßmann and Vorwerk 1995). Increasing moisture content decreases dehuller efficiency, and increases resistance of an oat to impact damage (Zorb and Hall 1960; Goncharova 1962; Bilanski 1966; Doehlert et al 1997).

Given constant impact dehuller efficiency, groat damage can vary among genotypes (Ganßmann and Vorwerk 1995). Functions of dehuller efficiency do not necessarily describe variation in groat damage. Doehlert et al (1999) studied groat damage and reported a positive correlation between groat damage caused by impact dehulling and groat content (the percentage of oat mass that is groat). Based on this relationship, the authors suggested that thick hulls, associated with lower groat content, might provide groats with more protection during dehulling. It is probably true that hulls provide protection during dehulling. The correlation suggests that primary kernels (with lower groat content) experience less groat damage during dehulling, which seems to contradict the Symons and Fulcher (1988) study because oat mass increases with kernel size (Murphy and Frey 1962; DeKoeyer et al 1993). However, the apparent contradiction may reflect different experimental approaches; the relationship is not clear. Progress in selection for groat content is attributed to changes in groat or hull mass, or both (Stuthman and Granger 1977; Ronald et al 1999).

Groat damage caused by impact dehulling is also likely due to a groat or hull effect, or both. These effects may be due to mass, but may also be due to fundamental mechanical behavior. Engleson and Fulcher (2002) showed that for constant groat mass and moisture content, other, undefined biological differences affected groat mechanical behavior. Knowledge of specific biological characteristics and how they influence mechanical behavior should lead to the prevention of groat damage during impact dehulling. Recent work (Doehlert and McMullen 2000) has accomplished this to some extent by modeling groat damage as a function of the single kernel characterization system (SKCS) hardness index, average groat mass for a 10-g groat sample (M_{10}), bran yield, and groat β -glucan content ($R^2 = 0.62$). Models of SKCS hardness index and bran yield also depended on groat damage, making it difficult to interpret the influence of groat characteristics on mechanical behavior. Doehlert and McMullen (2000) also reported significant correlations between SKCS hardness index and M_{10} and β -glucan content, and between bran yield and M_{10} , crude fat, β -glucan, and protein content. Other measures of groat characteristics and mechanical behavior may lead to improved models.

For example, groat bran is comprised of several layers: the outermost pericarp, followed by the testa, nucellus, and the aleurone layer (Fulcher 1986). Typically, the pericarp and aleurone layers are the thickest. Doehlert et al (1999) suggested that the hull might also prevent groat damage caused by impact dehulling. We

¹ Dept. of Food Science and Nutrition, University of Minnesota, St. Paul, MN 55108.

² Corresponding author. E-mail: gfulcher@umn.edu. Phone: (612) 626-1220. Fax: (612) 625-5272.

are not aware of any studies assessing the effect of the hull on groat damage. Therefore, one objective of this study is to develop a measure of hull mechanical behavior and determine whether variation in the mechanical behavior of the hull explains significant variation in groat damage caused by impact dehulling. The main objective of this study is to further develop interrelationships among specific groat characteristics, mechanical behavior, and damage caused by impact dehulling.

MATERIALS AND METHODS

Sample Preparation

Fifteen samples of oats (*Avena sativa* L.) were obtained from the Quaker Uniform Oat Nursery (Table I). Each sample was divided randomly by a riffle-style divider (model H-3985, Humboldt Testing Equipment, Norridge, IL) into 10-g samples. Samples were poured into a 0.5 L volume (V) and leveled using a filling hopper system (model 151, Seedburo Co., Chicago, IL), and test weight (oat mass/V) was calculated.

Wet Chemistry

Oat samples (10 g) were dehulled manually and groat mass (GM) was measured. Groats were then ground in a centrifugal Retsch mill (model ZM-1, Brinkman, Haan, Germany) through a 0.5-mm screen. Cell-wall phenolic acids were extracted as described by Sen et al (1991) with modifications detailed by McKeehen et al (1999). Phenolic acids (vanillic, caffeic, syringic, vanillin, coumaric, ferulic, and sinapic) were separated, identified, and quantified by HPLC analysis as described by McKeehen et al (1999). Starch and β -glucan contents were measured with commercial kits (Total Starch Assay Kit and Mixed-Linkage β -Glucan Test Kit, respectively, Megazyme, Wicklow, Ireland). Moisture, crude protein (Kjeldahl nitrogen \times 6.25), crude fat, and ash contents were determined according to Approved Methods 44-15A, 44-11, 30-25, and 08-01 (AACC 2000), respectively.

Compression Tests

Oat samples (10 g) were dehulled manually and sorted by groat mass into four subgroups: <0.02 g, 0.02–0.03 g, 0.03–0.04 g, and >0.04 g. Number fractions (N) were calculated for each subgroup. Maximum groat length and width were measured by digital image analysis using VideoPro (v. 3.2, Leading Edge Pty, Hove, S. A., Australia). Ten groats selected randomly from each subgroup were placed ventral side down on a copy stand with substage illumination. Images were captured with a Sony-89C CCD camera (model XC-77) with 512 \times 480 pixels/frame (0.1887 mm \times 0.2400 mm resolution) and a Tamron lens (F-28 mm).

TABLE I
Growing Location and Season of Genotypes Evaluated, and Genotype Sample Number^a

Location	Season	Genotype	Sample No.
Aberdeen, ID, USA	1997	MN93272	1
		0A974-1	2
		0A966-1	3
		86Ab4582	4
		0A970-10	5
Saskatoon, SK, CA	1997	Boyer	6
		Pacer	7
	1994	Derby	8
		Derby	11
		86Ab4582	12
	1996	Jerry	13
		S093221	14
0A971-2		15	
Ottawa, ON, CA	1996	AC Hunter	9
		0A952-3	10

^a Genotypes were coded numerically to simplify sample identification in figures.

Individual groats were compressed, and apparent stress and strain were calculated as described by Engleson and Fulcher (2002). Stiffness and toughness, two common material properties, were derived from the stress-strain curves. Apparent stiffness (S_{max}) was defined as the number average maximum of the first derivative of apparent stress (σ) with respect to apparent strain (ϵ), and was approximated using the secant line of the stress-strain points adjacent to point i

$$S_{max} = \sum_{k=1}^4 N_k \frac{\sum_{j=1}^{m_k} (\max \{S_i\})_{k,j}}{m_k} \approx \sum_{k=1}^4 N_k \frac{\sum_{j=1}^{m_k} \left(\max \left\{ \frac{\sigma_{i+1} - \sigma_{i-1}}{2\Delta\epsilon} \right\} \right)_{k,j}}{m_k} \quad (2)$$

where S_i is the first derivative at i , m is the number of compression tests completed (7–10) per subgroup k , and $\Delta\epsilon$ is the difference $\epsilon_i - \epsilon_{i-1}$. Apparent toughness (T) was defined as the number average definite integral of apparent stress from strain 0 to ϵ_{max} , and was approximated using the midpoint ($\bar{\epsilon}_i$) of $[\epsilon_{i-1}, \epsilon_i]$ and the Riemann sum

$$T = \sum_{k=1}^4 N_k \frac{\sum_{j=1}^{m_k} \left(\int_0^{\epsilon_{max}} \sigma(\epsilon) d\epsilon \right)_{k,j}}{m_k} \approx \sum_{k=1}^4 N_k \frac{\sum_{j=1}^{m_k} \left(\sum_{i=1}^n \sigma(\bar{\epsilon}_i) \Delta\epsilon \right)_{k,j}}{m_k} \quad (3)$$

where ϵ_{max} is the strain at maximum apparent stress and n is the number of midpoints from strain 0 to ϵ_{max} .

Impact Damage

Oat samples (10 g) were dehulled in an experimental impact dehuller (model L-92575, The Quaker Oats Co. Central Shop, Barrington, IL) with a 10.5 in. diameter finned distribution disk set at 3600 revolutions per minute. Output mass was sorted manually into 4 groups: undamaged groats (UG), oats (OT), hulls (H), and damaged groats (DG). OT were dehulled manually and their groat mass (GMot) was measured. Damaged groats were visibly split or cracked. In an attempt to account for variation in dehuller efficiency at constant dehuller speed, impact damage (ID) was defined as

$$ID = \frac{\text{percent of groat input mass that was damaged}}{\text{percent of groat input mass that retained hulls}} = \frac{GM - (UG + GMot)}{GMot} \quad (4)$$

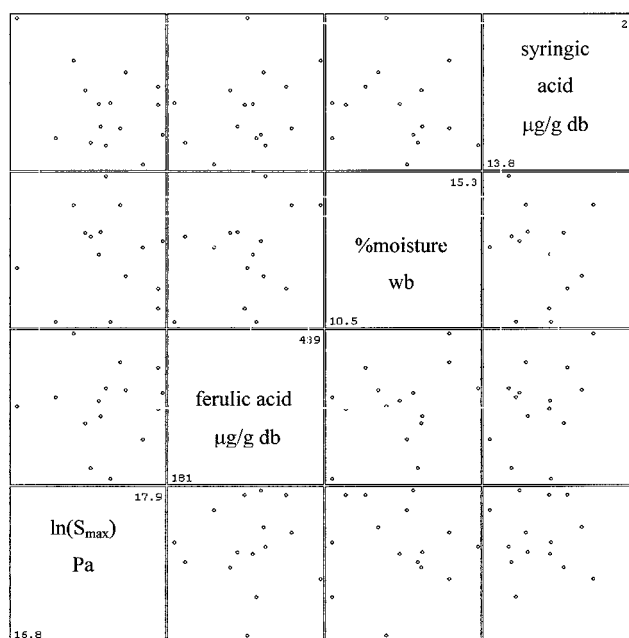


Fig. 1. Scatterplot matrix: apparent stiffness (S_{max}) model.

where GM is the groat mass obtained by dehulling manually 10 g of oat samples.

Pericarp and Aleurone Content

Estimates of pericarp and aleurone content (the percentage of groat sample that is pericarp and aleurone layer, respectively) were quantified by digital image analysis using the automated Dipix I440F microscope imaging system (measurement module Bran 14, v. 5.0, Dipix Technologies Inc., Ottawa, ON). This system is described in detail by Harrigan (1995). Samples (excluding sample 11 in Table I, which developed mold) were dehulled manually, ground in a centrifugal Retsch mill (model ZM-1, Brinkman, Haan, Germany) through a 0.5-mm screen, and packed in a sample holder (4 × 6 × 1 cm), which fit the microscope stage. Images (390 fields of view using a 2.5× objective) of fluorescent bran particles were captured with a monochrome 8-bit CCD camera and a 1.6× camera eyepiece. The filter combinations for pericarp content detection included an excitation filter (wavelengths [λ] 410–490 nm), a dichroic reflector (λ 505 nm), and a barrier filter (λ > 515 nm); the filter combinations for aleurone content detection included an excitation filter (λ 310–390 nm), a dichroic reflector (λ 380 nm), and a barrier filter (λ 410–490 nm).

Hull Damage

Because dehulling may cause permanent hull deformation, a measure of hull mechanical behavior was developed during the

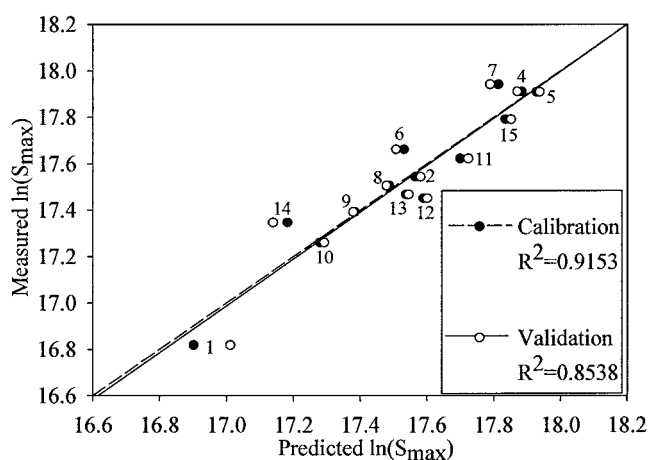


Fig. 2. Summary plot for partial least squares regression (PLSR): natural logarithm of apparent stiffness (S_{max}) Pa on ferulic acid $\mu\text{g/g}$ db, % moisture wb, and syringic acid $\mu\text{g/g}$ db.

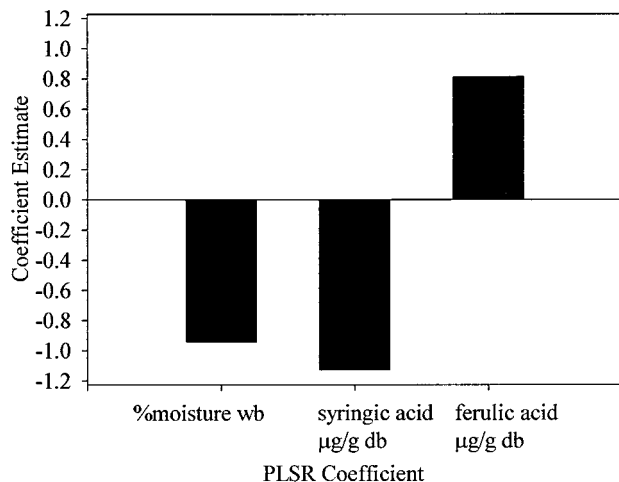


Fig. 3. Weighted partial least squares regression (PLSR) coefficients: natural logarithm of apparent stiffness (S_{max}) model.

dehulling process. Individual oats (10 g total, excluding sample 11 in Table I, which developed mold) positioned ventral side forward and distal end down were passed between experimental calendaring rolls (The Quaker Oats Company, Barrington, IL) with a 1-mm gap. The oat hull was compressed as it passed through the gap, which forced the groat from the hull. The groat remained on top of the rolls. Compression caused cracks and splits to form along the dorsal side of the hull, which were quantified by digital image analysis using Image-Pro Plus (v. 4.0, Media Cybernetics, Silver Spring, MD). Compressed hulls were placed ventral side down on a copy stand with substage illumination. Images were captured with a Sony-89C CCD camera (model XC-77) with 512 × 480 pixels/frame (0.1887 mm × 0.2400 mm resolution) and a Tamron lens (F-28 mm). Hull damage (HD) was calculated as

$$HD = \frac{(\text{crack and split area}) \times 100}{(\text{crack and split area}) + (\text{hull area})} \quad (5)$$

If hulls protect groats during impact dehulling, then perhaps hulls with low HD offer more protection during impact dehulling.

Statistical Analysis

Multiple linear regression (MLR) analysis was performed with Arc and the Xlisp-Stat system (v. 3.04, University of Minnesota, St. Paul, MN) using the least squares algorithm. Arc and MLR are described in detail by Cook and Weisberg (1999); the use of response and predictor transformations is a major theme of the text. Weighted MLR was used to model S_{max} and T. Weights were defined as the number of compression tests per sample (33–40). Samples lying outside the mean function ($P < 0.05$), based on the Bonferroni inequality as described by Cook and Weisberg (1999), were identified and discarded from analysis. Ordinary MLR was used to model impact damage.

Partial least squares regression (PLSR) was performed with Unscrambler (v. 6.11, CAMO ASA, Trondheim, Norway) using the PLS1 algorithm to model S_{max} , T, and ID. Initial PLSR variables were standardized to unit variance with the standard error of each variable. PLSR models were validated by full cross valida-

TABLE II
Weighted Multiple Linear Regression (MLR) Summary Statistics:
Natural Logarithm of Apparent Stiffness Model^{a-c}

Predictor	Regression Coefficient	Standard Error	<i>t</i>	<i>P</i>
y-Intercept	20.9697	0.3830	54.751	0.0000
Ferulic acid, $\mu\text{g/g}$ db	0.0036	0.0005	6.965	0.0000
%Moisture, wb	-0.2139	0.0265	-8.069	0.0000
Syringic acid, $\mu\text{g/g}$ db	-0.0910	0.0094	-9.705	0.0000

^a Sample 3 not included.

^b Response: $\ln(S_{max})$, where S_{max} has the unit Pa.

^c $R^2 = 0.9137$; $\sigma = 0.6074$; $df = 10$.

^d Overall analysis of variance regression values: df 3; SS 39.0748; MS 13.0249; $F = 35.30$; $P = 0.0000$.

^e Overall analysis of variance residual values: df 10; SS 3.6896; MS 0.3690.

TABLE III
Weighted MLR Summary Statistics:
Natural Logarithm of Apparent Toughness^{a-c}

Predictor	Regression Coefficient	Standard Error	<i>t</i>	<i>P</i>
y-Intercept	14.2536	0.2042	69.795	0.0000
(% β -glucan db) ⁻³	-47.9176	7.7834	-6.156	0.0001
(%protein db) ⁻²	-169.754	32.2436	-5.265	0.0003

^a Sample 9 not included.

^b Response: $\ln(T)$, where T has the units J/m^3 .

^c $R^2 = 0.8172$; $\sigma = 0.5274$; $df = 11$.

^d Overall analysis of variance regression values: df 2; SS 13.67948; MS 6.8395; $F = 24.59$; $P = 0.0001$.

^e Overall analysis of variance residual values: df 11; SS 3.0594; MS 0.2781.

tion. In general, each sample was treated successively as a prediction object, and prediction errors were combined in a validation model. Methods of validation and PLSR are described by Martens and Naes (1989). MLR may overfit noisy data compared to PLSR. However unlike PLSR, MLR is a method with tests of significance for the regression coefficients.

Scatterplot matrices were constructed with Arc. All other figures were constructed with SigmaPlot (v. 5.0, SPSS, Inc., Richmond, CA).

RESULTS AND DISCUSSION

Apparent Stiffness

The scatterplot matrix of the apparent stiffness model (Fig. 1) shows the marginal relationships between each pair of variables, without reference to the other variables. This is a visual lower bound for the goodness-of-fit that can be achieved with MLR (Cook and Weisberg 1999). The scatterplot matrix is a two-dimensional (2D) array of 2D plots. With the exception of the diagonal, each cell of the matrix contains a scatterplot. Variable names along the diagonal label the axes. Numbers along the diagonal are the minimum and maximum values of the variable in the cell. Plots above the diagonal are the transpose of plots below the diagonal. For example, the bottom right plot is the natural logarithm (ln) of S_{max} as a function of syringic acid, and the top left plot is syringic acid as a function of $\ln(S_{max})$. No strong linear or nonlinear trends are obvious, and no samples seem unusual in the scatterplot matrix.

Table II summarizes the weighted MLR of $\ln(S_{max})$ on the contents of ferulic acid, syringic acid, and moisture. Sample 3 was not included in the final MLR or PLSR analysis of S_{max} as it resided significantly outside the mean function. Sample 3 had the lowest moisture content (10.5% wb) of the 15 samples; sample 2 also had 10.5% moisture but did not seem unusual, suggesting that some other variable may make sample 3 different from the rest. Regression coefficients can be interpreted as the change in the expected response of $\ln(S_{max})$ given a change in the corresponding predictor of one unit, assuming that the other predictors in the model are constant (Cook and Weisberg 1999). For example, if moisture content is increased 1%, the expected decrease in $\ln(S_{max})$ is estimated to be 0.2139 units, assuming constant ferulic and syringic acid.

The standard error (Table II) of a regression coefficient (η) of the j th predictor (u_j) depends on the other predictors in the model and is defined as

$$se(\eta_j) = \frac{\hat{\sigma}}{se(u_j) \sqrt{n-1}} \sqrt{\frac{1}{1-R_j^2}} \quad (6)$$

where σ is the variance of the response in the subgroup with weight equal to 1, n is the number of samples, and R_j^2 is the coefficient of determination for the linear regression of u_j on the other predictors in the model (Cook and Weisberg 1999). If R_j^2 is close

to 1, then u_j is nearly equal to a linear combination of the other predictors and $se(\eta_j)$ is large; on the other hand, as R_j^2 approaches 0, $se(\eta_j)$ approaches a minimum value. R_j^2 either increases or stays the same as the number of predictors in the model increases (Cook and Weisberg 1999). Then increasing the number of predictors generally increases $se(\eta_j)$. Adding more predictors also changes the value and interpretation of each regression coefficient.

Tests of significance for the regression coefficients are listed in Table II. The t -value is the ratio of η_j to $se(\eta_j)$, and the p -value is the probability of observing a t -value at least as extreme as the one actually observed under the null hypothesis that η_j equals 0. Small p -values, like those in Table II, provide evidence against the null hypothesis. This evidence depends on $se(\eta_j)$ and, in turn, on the other predictors in the model. The coefficient of determination R^2 is the fraction of the variability in $\ln(S_{max})$ explained by adding the predictors to the model; 91% of the variability in $\ln(S_{max})$ is explained by adding the contents of ferulic acid, syringic acid, and moisture to the model of apparent stiffness. Table II also shows the overall analysis of variance as defined by Cook and Weisberg (1999), which suggests that a model without the predictors provides a much worse fit than that with the predictors.

Figure 2 is the PLSR summary plot for the apparent stiffness model; summary plots for MLR and PLSR were the same [$R^2(\text{Prediction}_{MLR}, \text{Prediction}_{PLSR}) > 0.9999$] for S_{max} , T, and ID models, and therefore only PLSR summary plots are presented. Calibration and validation lines for the apparent stiffness model (Fig. 2) are similar, and the coefficient of determination (R^2) is high for the calibration and validation cases (0.9153 and 0.8538, respectively) suggesting good model prediction ability. R^2 is the square of the sample correlation between the measured and predicted responses. R^2 is an appropriate measure of variability in this plot because the data form an elliptical cluster about the regression lines, and the deviations from the lines are constant.

Weighted PLSR coefficients are displayed in Fig. 3; the length of a bar indicates the relative importance of a variable and the direction indicates whether a variable has positive or negative influence on the response assuming that the other predictors in the model are constant. All three predictors are important in the model of apparent stiffness. Moisture content has negative influence on $\ln(S_{max})$; as moisture increases, $\ln(S_{max})$ decreases assuming fer-

TABLE IV
Ordinary MLR Summary Statistics:
Natural Logarithm of Impact Damage Model^{a-d}

Predictor	Regression Coefficient	Standard Error	t	P
y-Intercept	-29.5848	4.9369	-5.993	0.0001
(%moisture wb) ⁻²	1333.57	181.384	7.352	0.0000
%starch db	0.3548	0.0701	5.060	0.0004
(T/ S_{max}) ³	-1245173.0	331519.0	-3.756	0.0032

^a Response: $\ln(\text{ID})$.

^b $R^2 = 0.8491$; $\sigma = 0.9166$; $df = 11$.

^c Overall analysis of variance regression values: $df = 3$; $SS = 52.0252$; $MS = 17.3417$; $F = 20.64$; $P = 0.0001$.

^d Overall analysis of variance residual values: $df = 11$; $SS = 9.2424$; $MS = 0.8402$.

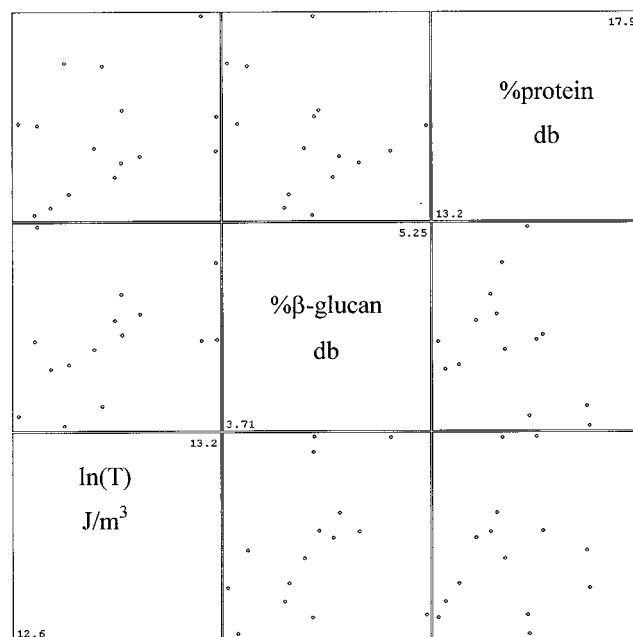


Fig. 4. Scatterplot matrix: apparent toughness (T) model.

ulic and syringic acid are constant. Research shows moisture plasticizes grain (Shpolayanskaya 1952; Zoerb and Hall 1960; Goncharova 1962; Bilanski 1966; Shelef and Mohsenin 1969; Husain et al 1971; Davison et al 1975; Herum et al 1979; Al Saleh and Gallant 1985; Pappas et al 1988; Dobraszczyk 1994; Bargale et al 1995; Bargale and Irudayaraj 1995) and plasticizers soften polymers in general (Sperling 1986) by decreasing inter- and intramolecular forces (Schmidt and Marlies 1948; Mohsenin 1986).

Ferulic acid has positive influence on $\ln(S_{max})$, and syringic acid has negative influence (Fig. 3). Ferulic acid esterifies with cell-wall polymers (Daniels et al 1963; Guenzi and McCalla 1966; Fulcher et al 1972; Harris and Hartley 1976; Durkee and Thivierge 1977; Hartley and Jones 1977; Fry 1979; Harris and Hartley 1980; Ring and Selvendran 1980; Fry 1982; Sosulski et al 1982; Smith and Hartley 1983; Collins 1986), which can be cross-linked by the oxidation of ferulate derivatives to diferulate cross-links (Hartley and Jones 1976; Markwalder and Neukom 1976; Neukom and Markwalder 1978; Harris and Hartley 1980; Fry 1983; Fry 1984; Shibuya 1984; Eraso and Hartley 1990). Such cross-linking decreases cell-wall extensibility (Fry 1983; Kamisaka et al 1990). The presence of a methoxy group at position 5 of syringic acid makes the formation of a disyringate cross-link unlikely. Polymers in general are cross-linked to prevent flow by producing a network (Sperling 1986). As the mass of a polymer network increases, noncovalent bonds holding it in place (as in the cell wall) become more effective (Schmidt and Marlies 1948; Fry

1983). Syringic acid or syringate derivatives may somehow decrease the effectiveness of such a network.

Apparent Toughness

Figure 4 contains the scatterplot matrix of the apparent toughness model. No strong linear or nonlinear trends are obvious in the scatterplot matrix. Sample 9 seems to stand apart from the other samples in the 2D plot of $\% \beta$ -glucan versus $\ln(T)$; sample 9 had the highest β -glucan content (5.25% db) and was considered to have high hull content (Burrows and McDiarmid 1993). Weighted MLR confirmed that sample 9 resided significantly outside the mean function, and it was not included in the final weighted MLR analysis presented in Table III or the PLSR results given in Figs. 5 and 6.

Regression coefficients (Table III) suggest that $\ln(T)$ increases as β -glucan content increases (assuming constant protein content) and as protein content increases (assuming constant β -glucan content). Tests of significance suggest that the regression coefficients in the apparent toughness model are not equal to zero, and the overall analysis of variance suggests that a model without the predictors provides a much worse fit than that with the predictors. The PLSR summary plot (Fig. 5) shows the data in an elliptical cluster about the calibration and validation regression lines, which are similar. There are no obvious trends in the deviations from the regression lines. The coefficient of determination is high for the calibration (0.8032) and validation (0.6957) cases suggesting prediction ability. The weighted PLSR coefficients (Fig. 6) suggest that both β -glucan and protein content are important in the apparent toughness model.

The composite cell wall is considered to be a primary source of toughening in plants (Lucas et al 2000). A mechanical composite is an organized mixture of two or more components, and a cell wall is known generally as fiber (Lucas et al 2000). β -glucan, a collective term for high molecular weight polymers of glucose linked by $\beta(1 \rightarrow 3)$ and $\beta(1 \rightarrow 4)$ glycosidic bonds (Fincher and Stone 1986), is a major hemicellulose in oat endosperm and aleurone cell wall (Wada and Ray 1978; Wood et al 1983). We are aware of disparities in terms of β -glucan (Wood et al 1983; Henry 1987; Miller and Fulcher 1994) and protein (Fulcher et al 1972; Youngs 1972; Bechtel and Pomeranz 1981) distributions across the grain, and so it would be premature to conclude that a single characteristic (or combination of characteristics) is causal.

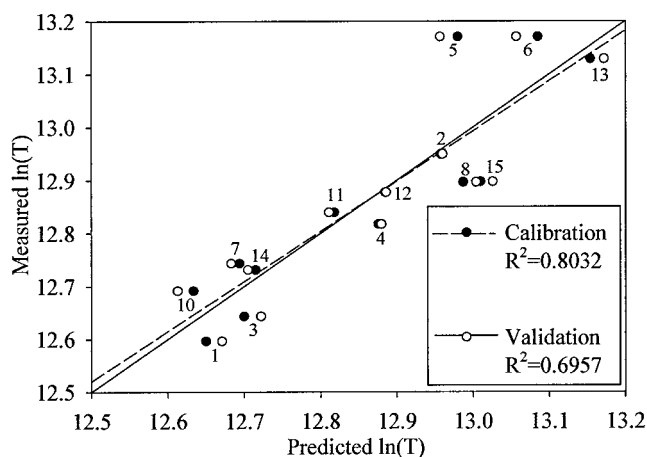


Fig. 5. Summary plot for partial least squares regression (PLSR): natural logarithm of apparent toughness (T) J/m^3 on $\% \beta$ -glucan db raised to the power of negative three $(\% \beta$ -glucan db) $^{-3}$ and $\%$ protein db raised to the power of negative two $(\% \text{protein db})^{-2}$.

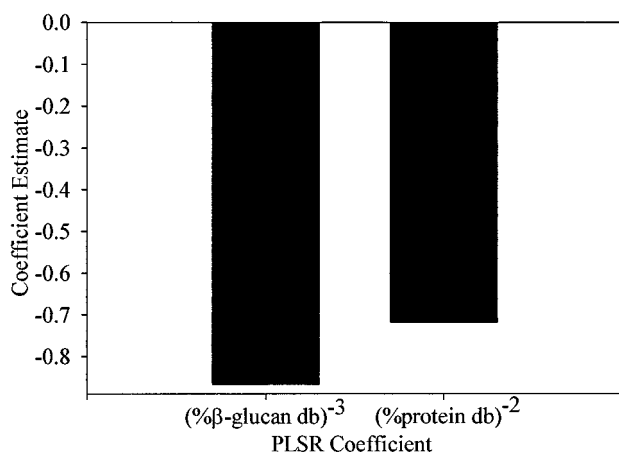


Fig. 6. Weighted partial least squares regression (PLSR) coefficients: natural logarithm of apparent toughness (T) model.

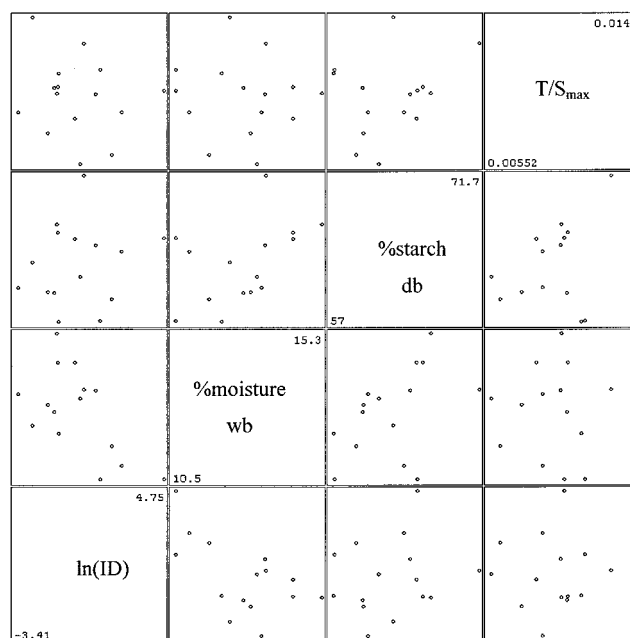


Fig. 7. Scatterplot matrix: impact damage (ID) model.

Impact Damage

Figure 7 contains the scatterplot matrix of the impact damage model. No strong linear or nonlinear trends are obvious, and no samples seem unusual in the scatterplot matrix. The MLR analysis of $\ln(\text{ID})$ on moisture content, starch content, and the ratio of T to S_{max} (T/S_{max}) is presented in Table IV. Tests of significance suggest that the regression coefficients are not equal to zero, and the overall analysis of variance suggests that a model without the predictors provides a much worse fit than that with the predictors. The PLSR summary plot (Fig. 8) shows the data in an elliptical cluster about the calibration and validation regression lines, which are similar. There are no obvious trends in the deviations from the regression lines. The coefficient of determination is high for the calibration (0.8491) and validation (0.7724) cases, suggesting prediction ability. The weighted PLSR coefficients (Fig. 9) suggest that all three predictors are important in the impact damage model.

Increasing moisture content appears to decrease impact damage, as does increasing T/S_{max} , assuming of course that the remaining predictors are constant. Adding moisture increases pliability and the ability to absorb impact energy, which has been demonstrated (Zoerb and Hall 1960; Goncharova 1962; Bilanski 1966; Doehlert et al 1997). Because a plasticizer works essentially by solvent action (Schmidt and Marlies 1948), cross-linkage among polymers reduces the modification effect of a plasticizer. The ratio T/S_{max} may reflect a cross-linking index because T is a function of polymer mass and S_{max} depends on the mass of cross-linking molecules. T/S_{max} is large when T is large or S_{max} is small. Then for low levels of impact damage the groat must be tough but not too stiff. The ratio of toughness to stiffness is an important parameter in the design of materials that can experience large displacement before failure (Ashby 1999; Lucas et al 2000).

Increasing starch content seems to increase impact damage under the assumption that moisture content and T/S_{max} are constant. Starch (like filler) may be stiffening the groat. In some materials, fillers interact with amorphous molecules, thereby serving as fix points that increase stiffness. These points are often more numerous and less strong than the covalent bonds that cross-link polymers (Schmidt and Marlies 1948). Fillers may also stiffen materials by forcing amorphous polymers to stretch partially around filler bodies, causing the material to work in a higher region of the stress-strain curve. There is usually little if any improvement in the elastic response of a filled material to external stress (Schmidt and Marlies 1948).

Addition of the predictor pericarp content squared, referred to as (pericarp content)², to the impact damage model in Table IV is also significant ($P_{(\text{pericarp content})^2} = 0.0211$, $R^2 = 0.9210$). If (pericarp

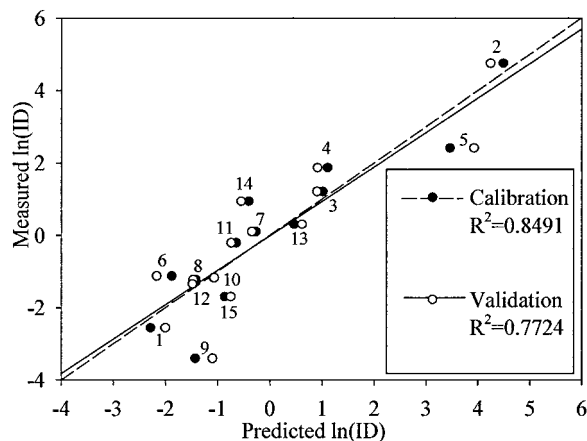


Fig. 8. Summary plot for partial least squares regression (PLSR): natural logarithm of impact damage (ID) on % moisture wb raised to the power of negative two ($\% \text{ moisture wb}^{-2}$), % starch db, and the ratio of apparent toughness to apparent stiffness cubed (T/S_{max}^3).

content)² is increased by one unit, the expected decrease in $\ln(\text{ID})$ is 0.4732 units, assuming that moisture content, starch content, and T/S_{max} are constant. This suggests that the pericarp layer provides groats with protection during impact dehulling. No significant ($P > 0.2$) $\ln(\text{ID})$ models are identifiable with aleurone content or HD as a predictor, suggesting that the aleurone layer and hull provide little if any protection to groats during impact dehulling. Because only 14 oat samples were evaluated (for aleurone content, pericarp content, and HD) and only one measure of hull damage was developed, results should be viewed with caution. Fluorescent material associated with aleurone content is likely part of the cell wall, and perhaps the germ, rather than the total aleurone layer. However, fluorescence analysis, as used in this study to estimate tissue content, is rapid and simple. The suggestion that pericarp content is an indicator of groat damage caused by impact dehulling might be exploited to identify cultivars with improved milling performance.

Test weight, crude fat, and ash were not important in models of groat apparent stiffness, apparent toughness, or impact damage for the samples evaluated. Given the small sample size, all results should be viewed with caution. Increasing genetic variability would probably result in more robust models; however, genetic extremes may be nonphysical or nonrelevant in the processing industry. Additionally, a statistically significant variable could be masking some unknown variable that actually explains the observed variation in the response.

CONCLUSIONS

Weighted MLR and PLSR of $\ln(S_{\text{max}})$ on the contents of ferulic acid, syringic acid, and moisture suggest that ferulic acid or perhaps diferulate cross-links increase groat stiffness, and that syringic acid or perhaps syringate derivatives and moisture decrease groat stiffness. Polymer cross-linking decreases extensibility, and moisture (a plasticizer) softens polymers. Weighted MLR and PLSR of $\ln(T)$ on β -glucan and protein content imply that both polymers increase groat toughness. β -glucan is a major cell-wall polymer, and plant cell walls confer toughness. The location of these polymers (perhaps concentrated in the bran) may also confer toughness. MLR and PLSR of $\ln(\text{ID})$ on moisture content, starch content, and the ratio T/S_{max} suggest that moisture content decreases impact damage (as does T/S_{max}), and starch content increases damage. Starch may act like filler, increasing stiffness and, in turn, damage by providing fix points or by forcing amorphous polymers to stretch around starch granules. Because T/S_{max} is large when T is large or S_{max} is small, groats must be tough but not too stiff for low levels of damage.

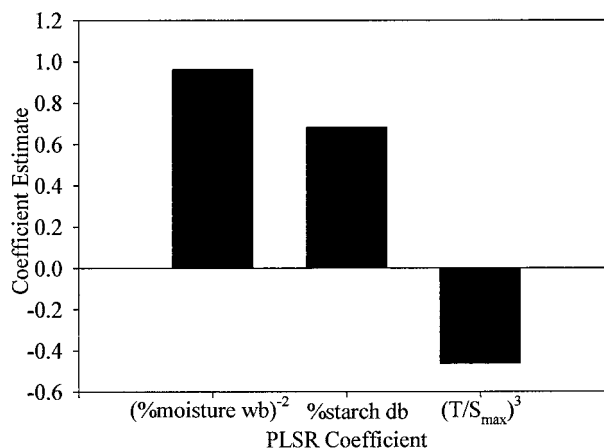


Fig. 9. Weighted partial least squares regression (PLSR) coefficients: natural logarithm of impact damage (ID) model.

ACKNOWLEDGMENTS

We are pleased to acknowledge that The Quaker Oats Company supported this research and appreciate the thoughtful statistical review from R. D. Cook.

LITERATURE CITED

- Al Saleh, A., and Gallant, D. J. 1985. Rheological and ultrastructural studies of wheat kernel behavior under compression as a function of water content. *Food Microstruct.* 4:199-211.
- American Association of Cereal Chemists. 2000. Approved Methods of the AACCC, 10th ed. The Association: St. Paul, MN.
- Ashby, M. F. 1999. Materials selection in mechanical design. Butterworth-Heinemann: Oxford.
- Bargale, P. C., and Irudayaraj, J. 1995. Mechanical strength and rheological behaviour of barley kernels. *Int. J. Food Sci. Technol.* 30:609-623.
- Bargale, P. C., Irudayaraj, J., and Marquis, B. 1995. Studies on rheological behavior of canola and wheat. *J. Agric. Eng. Res.* 61:267-274.
- Bechtel, D. B., and Pomeranz, Y. 1981. Ultrastructure and cytochemistry of mature oat (*Avena sativa* L.) endosperm. The aleurone layer and starch endosperm. *Cereal Chem.* 58:61-69.
- Bilanski, W. K. 1966. Damage resistance of seed grains. *Trans. ASAE* 9:360-363.
- Burrows, V. D., and McDiarmid, G. 1993. AC Hunter oat. *Can. J. Plant Sci.* 73:1099-1101.
- Collins, F. W. 1986. Oat phenolics: Structure, occurrence, and function. Pages 227-295 in: *Oats Chemistry and Technology*. F. H. Webster, ed. Am. Assoc. Cereal Chem.: St. Paul, MN.
- Cook, R. D., and Weisberg, S. 1999. Applied regression including computing and graphics. John Wiley and Sons: New York.
- Daniels, D. G. H., King, H. G. C., and Martin, H. F. 1963. Antioxidants in oats: Esters of phenolic acids. *J. Sci. Food Agric.* 41:385.
- Davison, E. F., Middendorf, J., and Bilanski, W. K. 1975. Mechanical properties of rapeseed. *Can. Agric. Eng.* 17:50-54.
- DeKoeyer, D. L., Stuthman, D. D., Fulcher, R. G., and Pomeranke, G. J. 1993. Effects of recurrent selection for grain yield on oat kernel morphology. *Crop Sci.* 33:924-928.
- Dobraszczyk, B. J. 1994. Fracture mechanics of vitreous and mealy wheat endosperm. *J. Cereal Sci.* 19:273-282.
- Doehlert, D. C., and McMullen, M. S. 2000. Genotypic and environmental effects on oat milling characteristics and groat hardness. *Cereal Chem.* 77:148-154.
- Doehlert, D. C., McMullen, M. S., Angelikousis, S., and Hareland, G. A. 1997. Factors affecting groat breakage and bran yield during oat milling. 3rd South American Oat Congress. Inia La Estanzuela: Colonia, Uruguay.
- Doehlert, D. C., McMullen, M. S., and Baumann, R. R. 1999. Factors affecting groat percentage in oat. *Crop Sci.* 39:1858-1865.
- Durkee, A. B., and Thivierge, P. A. 1977. Ferulic acid and other phenolics in oat seeds. *J. Food Sci.* 42:551-552.
- Engleson, J. A., and Fulcher, R. G. 2002. Mechanical behavior of oats: The groat effect. *Cereal Chem.* 79:787-789.
- Eraso, F., and Hartley, R. D. 1990. Monomeric and dimeric phenolic constituents of plant cell walls. *J. Sci. Food Agric.* 51:163-170.
- Fincher, G. B., and Stone, B. A. 1986. Cell walls and their components in cereal grain technology. Pages 278-295 in: *Advances in Cereal Technology*. Y. Pomeranz, ed. Am. Assoc. Cereal Chem.: St. Paul, MN.
- Fry, S. C. 1979. Phenolic components of the primary cell wall and their possible role in the hormonal regulation of growth. *Planta* 146:343-351.
- Fry, S. C. 1982. Phenolic components of the primary cell wall: Feruloylated disaccharides of D-galactose and L-arabinose from spinach polysaccharide. *Biochem. J.* 203:493-504.
- Fry, S. C. 1983. Feruloylated pectins from the primary cell wall: Their structure and possible function. *Planta* 157:111-123.
- Fry, S. C. 1984. Incorporation of [¹⁴C]cinnamate into hydrolase-resistant components of the primary cell wall. *Phytochemistry* 23:59-64.
- Fulcher, R. G., 1986. Morphological and chemical organization of the oat kernel. Pages 47-74 in: *Oats Chemistry and Technology*. F. H. Webster, ed. Am. Assoc. Cereal Chem.: St. Paul, MN.
- Fulcher, R. G., O'Brien, T. P., and Lee, J. W. 1972. Studies on the aleurone layer. I. Conventional and fluorescence microscopy of the cell wall with emphasis on phenol-carbohydrate complexes in wheat. *Aust. J. Biol. Sci.* 25:23-34.
- Fulcher, R. G., O'Brien, T. P., and Simmonds, D. H. 1972. Location of arginine-rich proteins in mature seeds of some Gramineae. *Aust. J. Biol. Sci.* 25:487-497.
- Ganßmann, W., and Vorwerk, K. 1995. Oat milling, processing, and storage. Pages 369-408 in: *The Oat Crop: Production and Utilization*. R. W. Welch, ed. Chapman and Hall: London.
- Goncharova, Z. 1962. Investigations into the effect of hydrothermal treatment of grain on the changes in its structural and mechanical properties. *Mukomol' no-elevatornia Promyshelen-nost.* 28:8-10.
- Guenzi, W. D., and McCalla, T. M. 1966. Phenolic acids in oats, wheat, sorghum, and corn residues and their phytotoxicity. *Agron. J.* 58:303-304.
- Handel, C. L. 2001. Agronomic and molecular study of tertiary kernels in oat using sister-line pairs. PhD dissertation. University of Minnesota: St. Paul, MN.
- Harrigan, K. 1995. Flour power: Microscopic image analysis in the food industry. *Cereal Foods World* 40:11-14.
- Harris, P. J., and Hartley, R. D. 1976. Detection of bound ferulic acid in the cell walls of Gramineae by ultraviolet fluorescence microscopy. *Nature* 259:508-510.
- Harris, P. J., and Hartley, R. D. 1980. Phenolic constituents of the cell walls of monocotyledons. *Biochem. Syst. Ecol.* 8:153-160.
- Hartley, R. D., and Jones, E. C. 1976. Diferulic acid as a component of cell walls of *Lolium multiflorum*. *Phytochemistry* 15:1157-1160.
- Hartley, R. D., and Jones, E. C. 1977. Phenolic components and degradability of cell walls of grass and legume species. *Phytochemistry* 16:1531-1534.
- Henry, R. J. 1987. Pentosan and (1→3), (1→4)-β-glucan concentrations in endosperm and wholegrain of wheat, barley, oats, and rye. *J. Cereal Sci.* 6:253-258.
- Herum, F. L., Mansah, J. K., Barre, H. J., and Majidzadeh, K. 1979. Viscoelastic behavior of soybean due to temperature and moisture content. *Trans. ASAE* 22:1219-1224.
- Husain, A. K., Agarwal, K., Ojha, T. P., and Bhole, N. G. 1971. Viscoelastic behavior of rough rice. *Trans. ASAE* 14:313-318.
- Kamisaka, S., Takeda, S., Takahashi, K., and Shibata, K. 1990. Diferulic and ferulic acid in the cell wall of *Avena* coleoptiles—Their relationships to mechanical properties of the cell wall. *Physiol. Plant.* 78:1-7.
- Lapveteläinen, A., Alho-Lehto, P., Sinn, L., Laukkanen, T., Lindman, T., Kallio, H., Kaitaranta, J., and Katajisto, J. 2001. Relationships of selected physical, chemical and sensory parameters in oat grain, rolled oats, and cooked oatmeal—A three-year study with eight cultivars. *Cereal Chem.* 78:322-329.
- Lucas, P. W., Turner, I. M., Dominy, N. J., and Yamashita, N. 2000. Mechanical defenses to herbivory. *Ann. Bot.* 86:913-920.
- Markwalder, H. U., and Neukom, H. 1976. Diferulic acid as a possible cross-link in hemicelluloses from wheat germ. *Phytochemistry* 15:836-837.
- Marshall, H. G., and Shaner, G. E. 1992. Genetics and inheritance in oat. Pages 509-572 in: *Oat Science and Technology*. H. G. Marshall and M. E. Sorrels, eds. ASA/CSA: Madison, WI.
- Martens, H., and Naes, T. 1989. Multivariate calibration. John Wiley and Sons: New York.
- McKeehen, J. D., Busch, R. H., and Fulcher, R. G. 1999. Evaluation of wheat (*Triticum aestivum* L.) phenolic acids during grain development and their contribution to *Fusarium* resistance. *J. Agric. Food Chem.* 47:1476-1482.
- Miller, S. S., and Fulcher, R. G. 1994. Distribution of (1→3),(1→4)-β-D-glucan in kernels of oats and barley using microspectrofluorometry. *Cereal Chem.* 71:64-68.
- Mohsenin, N. N. 1986. Physical properties of plant and animal material. Gordon & Breach Science Publishers: New York.
- Murphy, C. F., and Frey, K. J. 1962. Inheritance and heritability of seed weight and its components in oats. *Crop Sci.* 2:509-512.
- Neukom, H., and Markwalder, H. U. 1978. Oxidative gelation of wheat flour pentosans: A new way of cross-linking polymers. *Cereal Foods World* 23:374-376.
- Palagyi, A. 1983. Tertiary seed proportion in the grain yield of several oat varieties. *Cereal Res. Commun.* 11:269-274.
- Pappas, G., Skinner, G. E., and Rao, V. N. M. 1988. Effect of imposed strain and moisture content on some viscoelastic characteristics of cowpeas (*Vigna unguiculata*). *J. Agric. Eng. Res.* 39:209-219.
- Peek, J. M., and Poehlman, J. M. 1949. Grain size and hull percentage as factors in the milling quality of oats. *Agron. J.* 41:462-466.
- Pomeranz, Y., Davis, G. D., Stoops, J. L., and Lai, F. S. 1979. Test weight and groat-to-hull-ratios in oats. *Cereal Foods World* 24:600-602.

- Ring, S. G., and Selvendran, R. R. 1980. Isolation and analysis of cell wall material from beeswing wheat bran (*Triticum aestivum*). *Phytochemistry* 19:1723-1730.
- Ronald, P. S., Brown, P. D., Penner, G. A., Brule-Babel, A., and Kibite, S. 1999. Heritability of hull percentage in oat. *Crop Sci.* 39:52-57.
- Schmidt, A. X., and Marlies, C. A. 1948. *Principles of High-Polymer Theory and Practice*. McGraw-Hill: New York.
- Sen, A., Miller, S. S., Arnason, J. T., and Fulcher, R. G. 1991. Quantitative determination by HPLC and microspectrofluorimetry of phenolic acids in maize kernels. *Phytochem. Anal.* 2:225-229.
- Shelef, L., and Mohsenin, N. N. 1969. Effect of moisture content on mechanical properties of shelled corn. *Cereal Chem.* 46:242-253.
- Shibuya, N. 1984. Phenolic acids and their carbohydrate esters in rice endosperm cell walls. *Phytochemistry* 23:2233-2237.
- Shpolayanskaya, A. L. 1952. Structural-mechanical properties of the wheat grain. *Colloid J. (USSR)* 14:137-148.
- Smith, M. M., and Hartley, R. D. 1983. Occurrence and nature of ferulic acid substitution of cell-wall polysaccharides in graminaceous plants. *Carbohydr. Res.* 118:65-80.
- Sosulski, F., Krygier, K., and Hogge, L. 1982. Free, esterified, and insoluble-bound phenolic acids. 3. Composition of phenolic acids in cereal and potato flours. *J. Agric. Food Chem.* 30:337-340.
- Sperling, L. H. 1986. *Introduction to Physical Polymer Science*. John Wiley and Sons: New York.
- Stuthman, D. D., and Granger, R. M. 1977. Selection for caryopsis percentage in oats. *Crop Sci.* 17:411-414.
- Symons, S., and Fulcher, R. G. 1988. Relationship between oat kernel weight and milling yield. *J. Cereal Sci.* 7:215-217.
- Wada, S., and Ray, P. M. 1978. Matrix polysaccharides of oat coleoptile cell walls. *Phytochemistry* 17:923-931.
- Wesenberg, D. M., and Shands, H. L. 1971. Caryopsis percentage and related characters in early generations of *Avena sativa* L. *Crop Sci.* 11:586-588.
- Wood, P. J., Fulcher, R. G., and Stone, B. A. 1983. Studies on the specificity of interactions of cereal cell wall components with Congo red and Calcofluor. *J. Cereal Sci.* 1:95-110.
- Youngs, V. L. 1972. Protein distribution in the oat kernel. *Cereal Chem.* 49:407-411.
- Youngs, V. L., and Shands, H. L. 1974. Variation in oat kernel characteristics within the panicle. *Crop Sci.* 14:578-580.
- Zoerb, G. C., and Hall, C. W. 1960. Some mechanical and rheological properties of grains. *J. Agric. Eng. Res.* 5:83-93.

[Received July 6, 2001. Accepted July 2, 2002.]